

## Defects control for improved electrical properties in $(\text{Ba}_{0.8}\text{Sr}_{0.2})(\text{Zr}_{0.2}\text{Ti}_{0.8})\text{O}_3$ films by Co acceptor doping

Jun Miao, Khian Hooi Chew, and Yong Jiang

Citation: *Appl. Phys. Lett.* **99**, 232910 (2011); doi: 10.1063/1.3666021

View online: <http://dx.doi.org/10.1063/1.3666021>

View Table of Contents: <http://apl.aip.org/resource/1/APPLAB/v99/i23>

Published by the AIP Publishing LLC.

---

### Additional information on *Appl. Phys. Lett.*

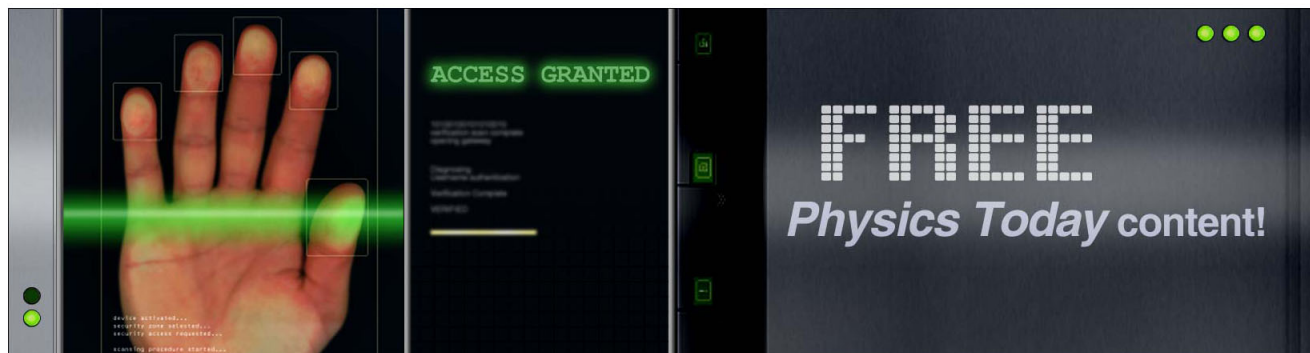
Journal Homepage: <http://apl.aip.org/>

Journal Information: [http://apl.aip.org/about/about\\_the\\_journal](http://apl.aip.org/about/about_the_journal)

Top downloads: [http://apl.aip.org/features/most\\_downloaded](http://apl.aip.org/features/most_downloaded)

Information for Authors: <http://apl.aip.org/authors>

## ADVERTISEMENT



# Defects control for improved electrical properties in $(\text{Ba}_{0.8}\text{Sr}_{0.2})(\text{Zr}_{0.2}\text{Ti}_{0.8})\text{O}_3$ films by Co acceptor doping

Jun Miao,<sup>1,a)</sup> Khian Hooi Chew,<sup>2</sup> and Yong Jiang<sup>1,b)</sup>

<sup>1</sup>State Key Laboratory for Advanced Metals and Materials, School of Materials Science and Engineering, University of Science and Technology Beijing, Beijing 100083, China

<sup>2</sup>Department of Physics, University of Malaya, 50603 Kuala Lumpur, Malaysia

(Received 5 July 2011; accepted 16 November 2011; published online 8 December 2011)

$(\text{Ba}_{0.8}\text{Sr}_{0.2})(\text{Zr}_{0.2}\text{Ti}_{0.8})\text{O}_3$  (BSZT) films were grown on  $\text{La}_{0.5}\text{Sr}_{0.5}\text{CoO}_3$  buffered (001)  $\text{SrTiO}_3$  substrates by pulsed laser deposition. Effects of Co doping on electrical properties of the films were investigated to establish material design through defects control. The doping led to a significant improvement in the electrical properties with reduction in leakage current and dielectric loss. In addition, the dielectric tunability and figure of merit were enhanced, implying that Co-doped BSZT films are promising materials for tunable microwave applications. Our detail studies suggest that the improved electrical properties of Co-doped BSZT films are closely related to defect concentrations in the films. © 2011 American Institute of Physics. [doi:10.1063/1.3666021]

Barium strontium titanate  $(\text{Ba,Sr})\text{TiO}_3$  (BST) has attracted considerable attention for their potential applications in microwave devices due to a high tunability under an external electric field.<sup>1–5</sup> As the tetravalent ions  $\text{Zr}^{4+}$  is chemically more stable than  $\text{Ti}^{4+}$ , barium zirconium titanate  $\text{Ba}(\text{Zr,Ti})\text{O}_3$  (BZT) has been chosen as an alternative to BST for tunable applications.<sup>6</sup> Many studies report that doping with small amount of acceptors such as  $\text{Er}^{3+}$ ,<sup>1</sup>  $\text{Mg}^{2+}$ ,<sup>2</sup>  $\text{Al}^{3+}$ ,<sup>3</sup>  $\text{Mn}^{2+}/\text{Mn}^{3+}$ ,<sup>4</sup> and  $\text{Co}^{2+}/\text{Co}^{3+}$  (Ref. 5) can greatly improve the electrical performance of BST films. Several studies have also investigated the effect of acceptor dopants such as  $\text{Ca}^{2+}$ ,<sup>7</sup>  $\text{Mg}^{2+}$ ,<sup>8</sup> and  $\text{Mn}^{2+}/\text{Mn}^{3+}$  (Ref. 9) on the electrical properties of BZT films.

In this letter, the effect of doping with low concentrations of Co on the dielectric and leakage properties of  $(\text{Ba,Sr})(\text{Zr,Ti})\text{O}_3$  (BSZT) films are investigated. Until now, the influence of Co dopants on the electrical properties of BSZT films has not been reported elsewhere. In this study, BSZT materials were chosen to utilize the high dielectric tunability of BST and the low dielectric loss of BZT.<sup>10</sup> In addition, Co acceptor dopant was chosen to suppress the ac/dc conductivities and improve the electrical properties of the films.

$(\text{Ba}_{0.8}\text{Sr}_{0.2})(\text{Zr}_{0.2}\text{Ti}_{0.8})_{1-x}\text{O}_3$  doped with  $\text{Co} = 0.0, 0.006, 0.013$  (abbreviated as BSZT0, BSZT6 and BSZT13) films are deposited *in-situ* on  $(\text{La}_{0.5}\text{Sr}_{0.5})\text{CoO}_3$  (LSCO) buffered (001)  $\text{SrTiO}_3$  substrate by pulsed laser deposition (PLD). A XeCl excimer pulsed laser ( $\lambda = 308 \text{ nm}$ ) of  $1.5 \text{ J/cm}^2$  and 3 Hz is used. The deposited temperature and oxygen pressure are controlled to be  $780^\circ\text{C}$  and 40 Pa, respectively. The thickness of BSZT:Co and LSCO layers are about 300 nm and 150 nm, respectively. After the depositions, the heterostructures are annealed at  $550^\circ\text{C}$  in oxygen ambient (1 atm) for 40 min. For electrical measurements, 200 nm Pt electrodes are deposited on the surface of the BSZT:Co/LSCO heterostructures through a metal shadow mask by sputtering.

Phase structures, surface morphologies, and electrical properties of the BSZT:Co thin films are investigated. Details of the measurements have been reported elsewhere.<sup>10</sup>

Figure 1(a) shows the  $\theta$ - $2\theta$  XRD patterns of the BSZT films on LSCO buffered (001) STO single crystals. Only the  $(h00)$  peaks of the BSZT:Co films and the  $(00l)$  peaks of the LSCO films are observed, indicating that those films grew perpendicular to the surface of STO substrate. Lattice parameters along the  $(h00)$  direction of the BSZT:Co thin films can be estimated from the  $(200)$  peaks ( $2d\sin\theta = \lambda$ ). The ionic radius of  $\text{Co}^{2+}$  ( $0.75 \text{ \AA}$ ) is larger than that of  $\text{Zr}^{4+}$  ( $0.72 \text{ \AA}$ ) and  $\text{Ti}^{4+}$  ( $0.61 \text{ \AA}$ ), but it is smaller than that of  $\text{Ba}^{2+}$  ( $1.35 \text{ \AA}$ ) and  $\text{Sr}^{2+}$  ( $1.18 \text{ \AA}$ ). The lattice parameter of the BSZT0, BSZT06, and BSZT13 are  $3.971 \text{ \AA}$ ,  $3.984 \text{ \AA}$ , and  $4.011 \text{ \AA}$ , respectively. An increase in the lattice parameter with increase of Co-concentration in the films implies that the  $\text{Co}^{2+}$  ions should be substituted into the B-site of  $\text{ABO}_3$  perovskite structures.

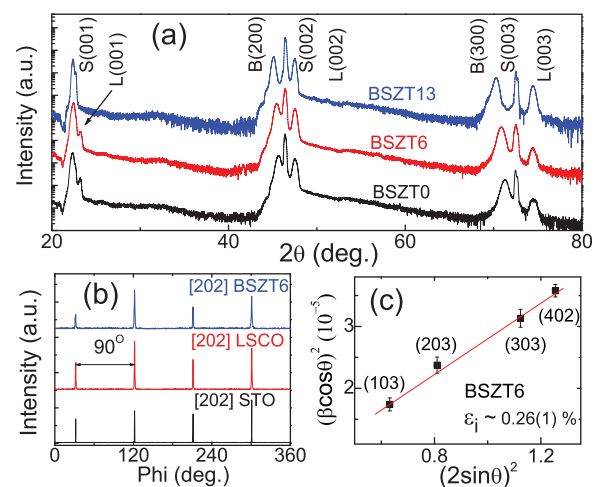


FIG. 1. (Color online) (a) XRD  $\theta$ - $2\theta$  patterns for all BSZT:Co films; (b)  $(202)$ -plane  $\Phi$  scan of 0.6 at% BSZT:Co film fabricated on LSCO buffered STO; (c) Williamson-Hall plot for analysis of inhomogeneous strains in 0.6 at% BSZT:Co film. The peaks are indexed as  $S$  for STO,  $B$  for BSZT, and  $L$  for LSCO, respectively.

<sup>a)</sup>Electronic mail: j.miao@ustb.edu.cn.

<sup>b)</sup>Electronic mail: yjiang@ustb.edu.cn.

Figure 1(b) shows the  $\varphi$ -scans of the BSZT6 (202), LSCO (202), and STO (202) reflections. The azimuthal diffraction patterns of the BZT6 film, LSCO bottom layer, and STO substrate clearly reveal the four-fold symmetry with the same orientation. No other peaks can be found in the intervals between those peaks, implying a highly oriented growth mode of BSZT6 and LSCO layers on STO substrate. Figure 1(c) depicts a typical Williamson-Hall plot for the 0.6% Co-doped BSZT films. Four planes (i.e., (103), (203), (303), and (402)) are selected for the William-Hall plots analysis<sup>11</sup>

$$(\beta \cos \theta)^2 = (K\lambda/D)^2 + (4\epsilon_i \sin \theta)^2, \quad (1)$$

where  $\beta$  is the measured diffractions peak width by subtracting the instrumental contributions;  $\theta$  is the diffraction angle;  $K$  is a geometrical constant close to 1;  $\lambda$  is the x-ray wavelength; and  $D$  is the coherence length along the scattering vector. The defect-induced inhomogeneous strain ( $\epsilon_i$ ) is extracted from the slope of linear fits of  $(\beta \cos \theta)^2$  as a function of  $(2\sin \theta)^2$ . According, the values of  $\epsilon_i$  are estimated to be  $0.31 \pm 0.02\%$ ,  $0.26 \pm 0.01\%$ , and  $0.17 \pm 0.01\%$  for BSZT0, BSZT6, and BSZT13 films, respectively. The result indicates a reduction of defect-induced inhomogeneous strain in the films due to the existence of Co-dopants.

In order to gain further insight on the effect of Co doping on the inhomogeneous strain in the BSZT films, we examine the ac electric-field dependence of dielectric constant at 1 MHz, as shown in Fig. 2. In the measurement, the samples were preliminarily polarized by cycling  $10^5$  times at 25 kV/cm to obtain a linear dielectric response.<sup>12</sup> Under subswitching fields, the domain-wall contribution to the dielectric permittivity  $\epsilon(E)$  can be examined by the Rayleigh law,<sup>13</sup>

$$\epsilon(E) = \epsilon_0 \epsilon_{init} + \alpha \epsilon_0 E, \quad (2)$$

where  $E$  ( $E < E_C$ ) is the applied ac field and  $E_C$  is the coercive field;  $\epsilon_0$  is the vacuum permittivity;  $\epsilon_{init}$  is the initial permittivity without external field; and  $\alpha$  is the Rayleigh coefficient due to the irreversible displacement of domain wall. Our study reveals that the Rayleigh coefficient  $\alpha$  of BSZT:Co films increases with increasing Co dopant concentration. A theory of Boser<sup>13</sup> indicates that the reciprocal of the Rayleigh coefficient  $\alpha^{-1}$  is proportional to the defect concentration, implying that the concentration of defects that

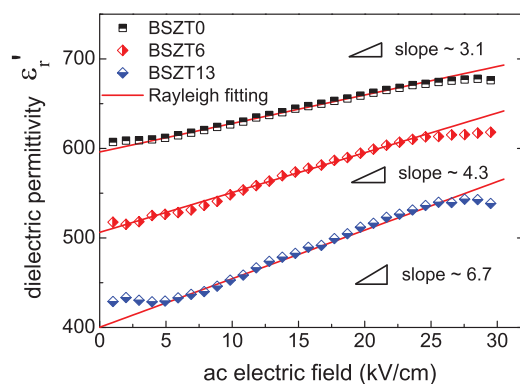


FIG. 2. (Color online) ac electric-field dependence of dielectric permittivity for BSZT:Co films under subswitching fields of 1 MHz measured at room temperature.

affecting the domain wall motion in BSZT films decreases with increase Co-dopant in the films.

The influence of Co-doping on the current density  $J$  versus electric field  $E$  characteristics of BSZT films is shown in Fig. 3(a). The leakage current in the undoped BSZT film is remarkably reduced upon addition of Co at each given electric field. Such a phenomenon is consistent with previous study that Co dopants can significantly decrease the leakage current in BST films.<sup>5</sup> Another interesting feature in Fig. 3(a) is that in different electric field regions, the Co-doping dependence of leakage current shows different characteristics. The bias polarity dependence of the  $J - E$  characteristics reveals that different leakage mechanisms operated in the positive and negative bias region.

Figure 3(b) shows the relationship of  $\ln(J/E) \sim E^{1/2}$  for BSZT:Co films under a positive bias, which can be divided into two regions corresponding to Poole-Frenkel (P-F) conduction and Fowler-Nordheim (F-N) tunneling regions. At a low field region, the leakage current can be characterized using the P-F conduction mechanism,<sup>14</sup>  $J_{PF} \sim E \exp[-(E_l/kT - e\sqrt{eE/\pi\epsilon_0\epsilon_{op}}/kT)]$ , where  $T$  is the temperature;  $E_l$  is the barrier height;  $k$  is the Boltzmann constant;  $e$  is the charge of an electron; and  $\epsilon_{op}$  is the optical dielectric permittivity. By extracting the optical dielectric constant from the slopes of the curves, the conduction mechanism can be identified. It is found that  $\epsilon_{op}$  range from  $3.8 \sim 5.6$  at  $E^{1/2} < 0.42$  MV/cm, which are quite close to the expected dynamic permittivity of BSZT films ( $\epsilon_{op} \sim 4$ ).<sup>15</sup> At the high field region,  $\epsilon_{op}$  deviates from the ideal value of  $\sim 4$  and follows the F-N tunneling behaviors,<sup>16</sup>  $J_{FN} \sim E^2 \exp(-4\sqrt{2}m^*(e\psi_0)^{3/2}/3e\hbar E)$ , where  $m^*$  is the effective electron mass; and  $\psi_0$  is the potential barrier height. A good fitting of leakage current data was found at  $E^{1/2} > 0.42$  MV/cm. Thus, the F-N tunneling appears as the dominant leakage current mechanism at the high field region due to electric-field concentration.

In Fig. 3(d), the  $\log J$  is plotted as a function of  $\log E$  for the leakage current data of BSZT:Co films for the negative bias region. The curves clearly show different slope regions for the  $J - E$  characteristics. It can be seen that all curves

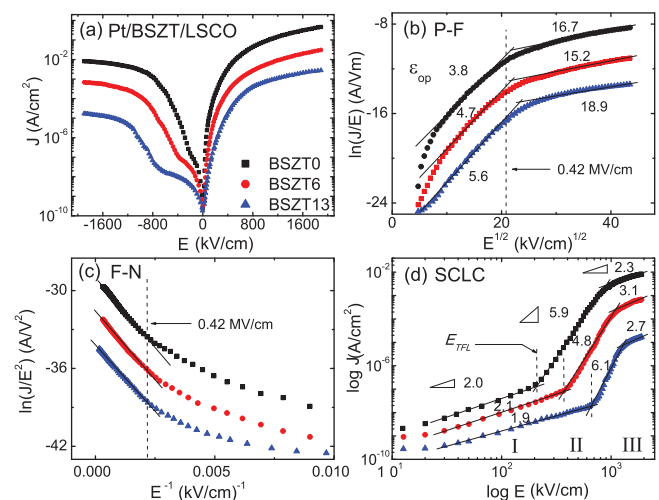


FIG. 3. (Color online) (a) Leakage current properties of BSZT:Co films with undoped, 0.6 at. %, and 1.3 at. % Co, respectively; (b) P-F; (c) F-N plots of BSZT:Co films under a positive bias; (d)  $\log J$  versus  $\log E$  plots of BSZT:Co films under an negative bias.

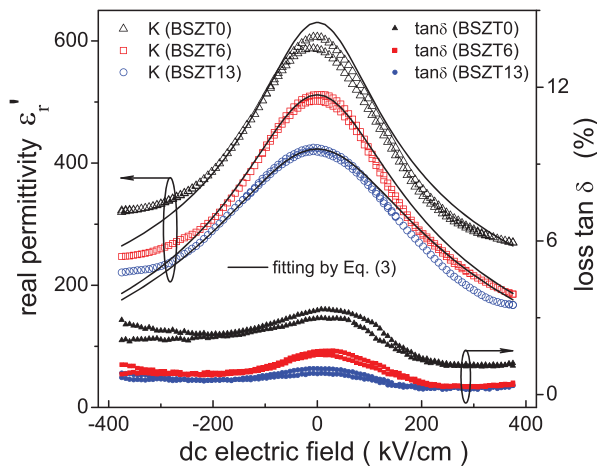


FIG. 4. (Color online) dc electric-field dependence of dielectric permittivity and loss tangent for BSZT:Co films measured at 1 MHz. The solid lines indicate the fitting results by Johnson's [Eq. (3)].

follow a space-charge-limited (SCL) conduction behavior, which is expressed as<sup>17</sup>  $J_{SCLC} = 9\epsilon_r\epsilon_0\theta\mu E^2/8d$ , where  $\epsilon_r$  is the permittivity of the insulator;  $\mu$  is the free electron mobility; and  $d$  is the film thickness. At the low bias region I, the slopes of  $\log J \sim \log E$  curve are all close to 2, indicating a transition from Ohmic to SCL behaviors. With increasing electric fields, a transition region characterized by a large slope of  $\sim 5-6$  is seen (region II). Upon further increasing, the electric field, the slopes of  $J-E$  curves change to about 2-3 again (region III). The deviations of the slope in regions I and III can be attributed to the scattered distribution of the trapping levels because of structural and chemical disorders in the films.<sup>18</sup>

Now we explore the possible applications of these materials in tunable microwave applications. Figure 4 shows the dc electric-field  $E_{dc}$  dependence of dielectric permittivity  $\epsilon_r'$  and loss  $\tan \delta$  measured at 1 MHz and 200 mV. Although  $\epsilon_r'$  decreases with increasing Co content, the loss  $\tan \delta$  at zero electric field of the films were improved. For example, the  $\tan \delta$  of BSZT0, BSZT6, and BSZT13 films are 0.036, 0.017, and 0.0097, respectively. The relationship between dielectric permittivity and dc electric field is given by the Landau-Devonshire theory as<sup>19</sup>

$$\epsilon_r(E) = \frac{\epsilon_r(0)}{[1 + 3\beta\epsilon_0^3\epsilon_r^3(0)E^2]^{1/3}}, \quad (3)$$

where  $\beta$  is the Landau parameter;  $\epsilon_r(0)$  and  $\epsilon_r(E)$  are the dielectric permittivity at zero and applied electric field  $E$ , respectively. The values of  $\beta$  for BSZT0, BSZT6, and BSZT13 samples are estimated to be  $2.7 \times 10^{10}$ ,  $5.3 \times 10^{10}$ , and  $9.1 \times 10^{10} \text{ m}^5\text{F}^{-3}\text{V}^{-2}$ , respectively. The dielectric tunability is defined as  $\eta = |\epsilon_r(0) - \epsilon_r(E)|/\epsilon_r(0)$  and the figure of merit (FOM) can be obtained using  $\text{FOM} = \eta/(\tan \delta)_{\text{max}}$ .

It is found that the dielectric tunability (@375 kV/cm) of BSZT0, BSZT6, and BSZT13 samples are 54.5%, 69.1%, and 63.7%, respectively, and the FOM are 15.1, 38.5, and 65.7, respectively. The result shows that a small quantity of Co can improve the tunable properties in BSZT films.

In summary, Co-doping has been shown to be an efficient way to improve the electrical properties of the BSZT films. Changes in inhomogeneous strains in BSZT films caused by Co doping were investigated through the W-H plot analysis. The dependence of Rayleigh coefficient under subswitching fields on the doping concentration was examined. The leakage current properties were investigated by systematically studying the  $J-E$  characteristics under positive and negative biases. This study suggest that the defects concentrations is responsible for the improved electrical properties in the BSZT:Co films.

This work was partially supported by the NSFC (Grant Nos. 50802007, 50831002, 11174031, and 51071022), the National Basic Research Program of China (Grant No. 2012CB932702), the RFD of Higher Education of China (Grant No. 200800081011), and Fok Ying-Tong Education Foundation (Grant No. 121046).

- <sup>1</sup>J. L. Wang and S. Trolrier-McKinstry, *Appl. Phys. Lett.* **89**, 172906 (2006).
- <sup>2</sup>M. W. Cole, E. Ngo, S. Hirsch, M. B. Okatan, and S. P. Alpay, *Appl. Phys. Lett.* **92**, 072906 (2008).
- <sup>3</sup>K. B. Chong, L. B. Kong, L. Chen, L. Yan, C. Y. Tan, T. Yang, C. K. Ong, and T. Osipowicz, *J. Appl. Phys.* **95**, 1416 (2004).
- <sup>4</sup>M. Jain, S. B. Majumder, R. S. Katiyar, F. A. Miranda, and F. W. Van Keuls, *Appl. Phys. Lett.* **82**, 1911 (2003).
- <sup>5</sup>S. Y. Wang, B. L. Cheng, C. Wang, S. Y. Dai, H. B. Lu, Y. L. Zhou, Z. H. Chen, and G. Z. Yang, *Appl. Phys. Lett.* **84**, 4116 (2004).
- <sup>6</sup>P. W. Rehrig, S. E. Park, S. Trolrier-McKinstry, G. L. Messing, B. Jones, and T. R. Shrout, *J. Appl. Phys.* **86**, 1657 (1999); A. Dixit, S. B. Majumder, R. S. Katiyar, and A. S. Bhalla, *Appl. Phys. Lett.* **82**, 2679 (2003).
- <sup>7</sup>N. Cramer, E. Philofsky, L. Kammerdiner, and T. S. Kalkur, *Appl. Phys. Lett.* **84**, 771 (2004).
- <sup>8</sup>W. C. Yi, T. S. Kalkur, E. Philofsky, L. Kammerdiner, and A. A. Rywak, *Appl. Phys. Lett.* **78**, 3517 (2001).
- <sup>9</sup>W. J. Jie, J. Zhu, W. F. Qin, X. H. Wei, J. Xiong, Y. Zhang, A. Bhalla, and Y. R. Li, *J. Phys. D* **40**, 2854 (2007).
- <sup>10</sup>J. Miao, J. Yuan, H. Wu, S. B. Yang, B. Xu, L. X. Cao, and B. R. Zhao, *Appl. Phys. Lett.* **90**, 022903 (2007); J. Miao, H. Y. Tian, X. Y. Zhou, K. H. Pang, and Y. Wang, *J. Appl. Phys.* **101**, 084101 (2007).
- <sup>11</sup>G. Catalan, B. Noheda, J. McAneney, L. J. Sinnamon, and J. M. Gregg, *Phys. Rev. B* **72**, 020102 (2005).
- <sup>12</sup>D. V. Taylor and D. Damjanovic, *Appl. Phys. Lett.* **76**, 1615 (2000).
- <sup>13</sup>O. Boser, *J. Appl. Phys.* **62**, 1344 (1987).
- <sup>14</sup>J. Frenkel, *Tech. Phys. USSR* **5**, 685 (1938).
- <sup>15</sup>A. Y. Liu, J. Q. Xue, X. J. Meng, J. L. Sun, Z. M. Huang, and J. H. Chu, *Appl. Surf. Sci.* **254**, 5660 (2008); S. T. Chang and J. Y. Lee, *Appl. Phys. Lett.* **80**, 655 (2002).
- <sup>16</sup>L. Pintilie, I. Vrejoiu, D. Hesse, G. Lerhun, and M. Alexe, *Phys. Rev. B* **75**, 104103 (2007).
- <sup>17</sup>M. A. Lampert and P. Mark, *Current Injection in Solids* (Academic, New York, 1970), p. 27.
- <sup>18</sup>C. J. Peng and S. B. J. Krupanidhi, *Mater. Res.* **10**, 708 (1995).
- <sup>19</sup>K. M. Johnson, *J. Appl. Phys.* **33**, 2826 (1962).